A COMPREHENSIVE REVIEW OF CHROMITE, FERRITE AND ALUMINATE NANO-MATERIALS

Gajanan B. Dhake[1*], Shalini T. Dengle[2], Ravindra S. Dhivare[3]

[1]Department of Chemistry, Yashwantrao Chavan College of Science, Karad, Maharashtra, India*
[2]Department of Chemistry, Vivekanand Arts, Sardar Dalipsingh Commerce & Science College Samarthanagar, Aurangabad, Maharashtra, India
[3]Department of Chemistry, BSSPMs Arts, Commerce & Science College, Songir, Dhule, Maharashtra, India

Abstract: *Spinel oxides, which have the general formula AB_2O_4, are durable materials that may be used for a variety of processes, including catalysis. The distribution of various cations in the A and B sites is mostly influenced by the stabilization of respective crystal fields. This distribution's impact on the catalytic characteristics is not insignificant. Octahedral B sites are more exposed than tetrahedral A sites when the spinel structure is broken by a surface. However, with the comparison of chromite, ferrite, and aluminates oxides is exciting - this provides researchers an opportunity to really understand the differences between them and how they react under different circumstances! Chromite oxide has a high temperature coefficient of electrical resistance and provides electrical insulation up to 500°C. On the other hand, ferrite oxide demonstrates good magnetic properties including low power loss in various magnetic applications. Last but not least, aluminates are ideal for use in optoelectronics since they mostly consist of aluminium and numerous metal oxides. Aluminates have a lower thermal conductivity than the majority of metals, which makes them superior in this regard. Now with these three oxides at our study, the researchers are able to investigate a virtually infinite number of possibilities, each one of which may ultimately lead us to new discoveries that make life easier.*

Keywords: ***nano-materials, metal oxides, chromite, ferrites, aluminates***

1. INTRODUCTION

In recent years, the development of nano materials has garnered a significant amount of attention across various fields of study. In this essay, we will perform a full review of ferrite, chromite, and aluminate nano materials. A lot of research has been carried out on the synthesis and characterization of ferrite chromite and aluminate nano materials capable of being used in various fields of science and engineering. These materials exhibit remarkable magnetic, electrical, thermal, and catalytic properties. They are known to be efficient in many industrial applications, making them highly valuable substances to researchers and industries across the globe.

Ferrites are a class of ceramic materials that display magnetic properties, making them useful in various applications such as magnetic storage media, microwave devices, and sensors. Ferrite nano materials have been extensively studied due to their unique properties, including high magnetic anisotropy and improved magnetic responsiveness. Ferrite nano materials can be synthesized using various methods, including sol-gel processing, co-precipitation, and hydrothermal synthesis. The properties of ferrite nano materials can be easily tuned by controlling the synthesis parameters such as temperature, pH, and precursor concentration. Some of the current applications of ferrite nano materials include magnetic resonance imaging, drug delivery systems, and environmental remediation.

Chromite nano materials are another class of materials that have gained significant attention in recent years, mainly due to their unique properties, including high thermal stability, tuneable electrical and magnetic properties, and high refractive index. Chromite nano materials can be synthesized using various techniques, including sol-gel processing, hydrothermal synthesis, and co-precipitation, with the desired properties dependent on the synthesis method used. Chromite nano materials have applications in various fields, including energy conversion, catalysis, and biomedical imaging. For example, chromite nano materials are used as catalysts in the production of hydrogen fuel from water.

Aluminate nano materials are another class of ceramic materials that have unique properties, including thermal stability, high hardness, and high refractive index.

Corresponding Author: *Gajanan B. Dhake*

Aluminate nano materials can be synthesized using various techniques, including sol-gel processing, hydrothermal synthesis, and co-precipitation, with properties dependent on the synthesis method used. Aluminate nano materials have applications in various fields, including catalysis, energy conservation, and electronic devices. For example, aluminate nano materials can act as catalysts for the conversion of carbon dioxide into valuable products such as methanol.

2. Spinel system of the mixed metal oxides

Spinels with the nanomaterials of mixed metal oxides are a true marvel of modern materials science. They possess an extraordinary combination of physical, chemical, and electronic properties that make them ideal for a diverse range of applications. These spinels have a unique crystalline structure that results in exceptional mechanical strength, high thermal stability, and outstanding electrical conductivity. Furthermore, their surface area-to-volume ratio is extremely high due to the presence of nanoscale features, which makes them excellent candidates for catalysis and energy storage devices. Spinels with mixed metal oxides offer unprecedented flexibility in tailoring their properties to meet the specific demands of various applications. In short, these spinels are invaluable building blocks for creating advanced technologies that will drive progress in industries ranging from electronics to biomedicine. Spinels with the formula AB_2O_4 (where A and B are metal ions) and the properties of magnetism, optics, electricity, and catalysis had already taken on prominent roles in applications of data storage, biotechnology, electronic devices, lasers, sensors, conversion reactions, and energy storage or conversion. Improved ORR/OER catalytic activity produced by this control may be used in fuel cells, metal-air batteries, and water-splitting devices to boost their performance characteristics. The success of these applications is largely dependent on the exact structures and physical and chemical properties of the spinels [1].

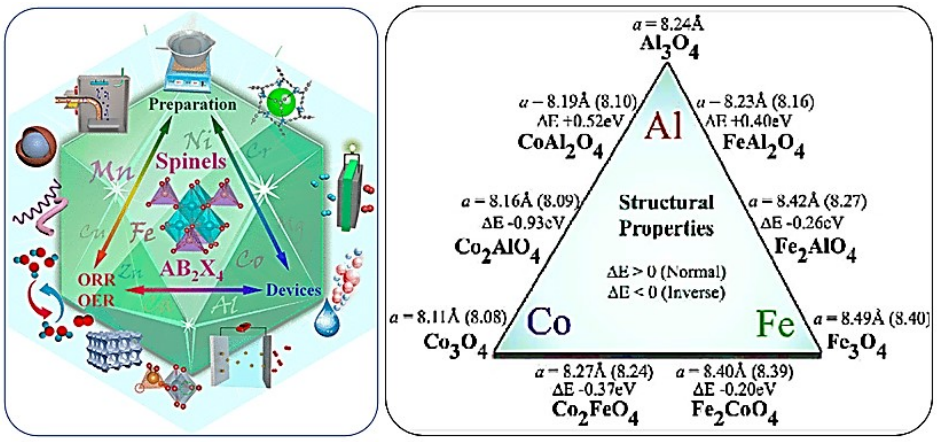

Fig 1: Preparation, morphology, physicochemical and calculated structural features of spinels [1,2]

To get crystalline chromites, ferrites and aluminate spinels with microscopic particle size, many methods of preparation are being investigated, including co-precipitation, sol-gel synthesis, sono-chemical approach, microwave heating, and chemical compound mixing route. Wet chemical techniques were motivated by the critical necessity for well-controlled homogeneity and high-purity materials. The combustion pathway is a key strategy for preparing chromites, ferrites and aluminates. The benefit of the solution combustion process is that the element cations are dispersed quasi-atomically in liquid precursors, allowing for the production of crystalline powder with low particle size and good purity at low temperatures [3-14].

3. Method of synthesis of chromite, ferrite and aluminate mixed metal oxides

There are several types of synthesis methods available for producing mixed metal oxide spinels, including solid-state reaction, co-precipitation, hydrothermal method, microwave method, sol-gel method and so on. The choice of the method depends on the desired properties and applications of the material. Solid-state reactions involve heating precursor materials in a furnace to initiate a chemical reaction leading to a crystalline product. Co-precipitation involves precipitation of multiple metallic ions together in solution followed by calcination. Hydrothermal and sol-gel methods both involve controlled growth of crystalline materials at lower temperatures using specific precursors in solution or gel form. Each method has its own advantages and disadvantages regarding process control, scalability, reproducibility, purity and ease-of-handling. A deep understanding and selection of the appropriate synthesis technique can result in efficient fabrications suitable for electronic devices, catalysis or energy applications.

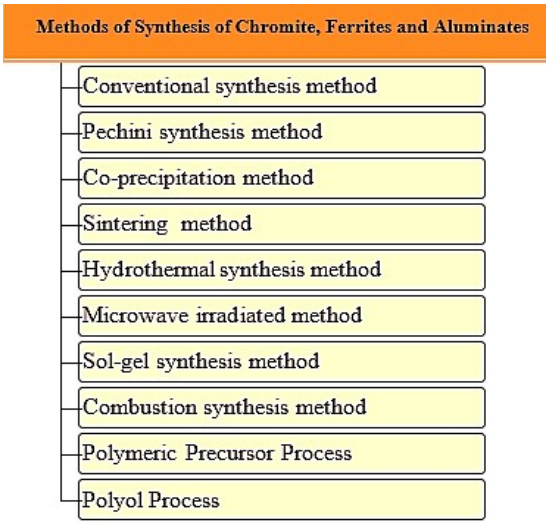

Fig. 2: Method of synthesis of mixed metal oxides

4. Comprehensive Reviews of Chromites, Ferrites and Aluminates

1.1 CHROMITES:

Abdolmohammadi and Dahi-Azar Copper chromite nanoparticles ($CuCr_2O_4$ NPs) were made hydrothermally in this study. This nanomaterial produced a new family of benzopyran azo colours as a heterogeneous magnetic catalyst. In a pseudo-three-component synthesis, (E)-1,2-diphenyl1-diazene and 4-hydroxycoumarin were mixed 1:2. This study developed a viable, high-yield methodology with multiple benefits. Benefits include a simple technique with easy work-up, mild reaction conditions, and the use of $CuCr_2O_4$ NPs as an effective and recoverable catalyst [15].

Safaei-Ghomi, J. et al. created a simple and efficient C-N cross coupling reaction of anilines and aryl halides utilising $CuCr_2O_4$ nanoparticles as a heterogeneous catalyst under ligand-free conditions. A powerful heterogeneous catalyst is used. Recycling the catalyst gives triarylamines quickly. The environment was unaffected by moderate weather. $CuCr_2O_4$ nanoparticles enabled ligand-free, feasible, efficient, and effective C-N coupling between anilines and aryl iodides. SEM, IR, and X-ray diffraction were

employed to fully describe the heterogeneous catalyst. This ligand-free approach uses $CuCr_2O_4$ nanoparticles for recycling, high product yields, and fast reaction times [16].

Shojaei A.F. et al. This research developed sol-gel $CuCr_2O_4$ and $CuCr_2O_4/TiO_2$ nanocomposites with regular spinel architectures. These nanocomposites were examined for alcohol oxidation catalysis and structure. Without catalysts or oxidants, alcohol did not oxidise. Catalysis under reflux settings is substantially more active than under light irradiation response. TiO_2 broad band gap facilitates electron-hole separation when coupled with $CuCr_2O_4$, a semiconductor with a tiny band gap $CuCr_2O_4/TiO_2$ heterojunction coupling improves catalytic activity [17].

Saeed, M. et al. have been successfully created chromite spinels Co1-xNixCr_2O_4 (x = 0-1 with a step size of 0.2), synthesis techniques were used. Cobalt-chromium spinel $CoCr_2O_4$ and nickel-doped chromates were produced in a single phase at a range of calcination temperatures (600-700℃). Ni-substituted chromates, on the other hand, were discovered to have phase compositions that varied with annealing temperature. Spinel-type and simple oxide crystalline phases were found in these samples at higher substitution ratios of 0.6 and 1. Increasing the Ni dopant concentration causes the Co peak to disappear. Significant optical device and improved photocatalytic applications highlighted the significance of these research [18].

Acharyya, S. S. et al. demonstrated the surfactant-mediated hydrothermal production of a $CuCr_2O_4$ spinel nanoparticle catalyst that selectively oxidised aniline to azoxybenzene. XRD, XPS, SEM, TEM, TGA, and ICP-AES characterised the catalyst. HRTEM showed that the catalyst is formed of 35-nm-sized homogeneous particles. At 70℃ degrees Celsius, H_2O_2 can convert 78% of aniline into azoxybenzene with 92% selectivity. The catalyst did not drain after five reuses, proving its heterogeneity. Our freshly constructed $CuCr_2O_4$ spinel nanoparticle catalyst could catalyse aniline to azoxybenzene in one step [19].

Kawamoto A.M. et al. Copper chromite ($CuCr_2O_4$) catalysts were synthesised by ceramic and coprecipitation methods and studied by X-ray diffraction, SEM, elemental, differential calorimetric (DSC), thermogravimetric, granulometric, mass, and infrared spectroscopy (IR). The coprecipitation samples' DSC, SEM, and X-ray characteristics differed. DSC demonstrated a tetragonal cubic phase transition, SEM showed particles with definite crystalline forms, and X-ray analysis identified $CuCr_2O_4$. Burning rate and mechanical qualities were measured for $CuCr_2O_4$-containing HTPB propellants. Iron (III) oxide-catalysed HTPB propellants were compared. Coprecipitation-synthesized samples with a more defined crystalline structure had the highest combustion rates [20].

Safaei-Ghomi, J. et al. has been utilised the $CuCr_2O_4$ nanoparticles as a ligand-free, highly efficient heterogeneous catalyst for the C-N cross coupling reaction of anilines and aryl halides, resulting in a straightforward and effective approach. The catalyst is reusable and produces high-quality triarylamines with rapid turnover. Environment was quite gentle, neutral, and benign. Using $CuCr_2O_4$ nanoparticles, the C-N coupling process between anilines and aryl iodides were carried out in a streamlined, productive, and ligand-free manner. The production of triarylamines was sped up and simplified with the use of a copper chromite nano catalyst. Scanning electron microscopy, infrared analysis, and X-ray diffraction were all used to determine the precise nature of the heterogeneous catalyst. The significant benefits of this ligand-free approach using $CuCr_2O_4$ nanoparticles include their recyclability, good yields of products, and short reaction times [21].

Manoharan S.S. and Patil K. C. have been investigated the fine-particle metal chromites (MCr_2O_4, where M = Mg, Ca, Mn, Fe, Co, Ni, Cu, and Zn) is prepared in stoichiometric quantities by combustion of aqueous solutions comprising the respective metal nitrate, chromium (III) nitrate, and urea. The mixtures ignite and generate voluminous chromites with surface areas varying from 5-25 m^2/g when rapidly heated to 35℃ [22].

Zhigaikina I. A. et al. has been demonstrated sol-gel system taken into consideration for the synthesis of lanthanum chromite. Investigation is done into how the temperature, duration, and quantity of the heat treatment affect how quickly the synthesis is

completed. The procedure' ideal parameters are stated. It is shown that it is possible to make small ceramic items by substituting powder made by the sol-gel technique for powder made by vibration crushing electrically molten lanthanum chromite [23].

Youn Y. et al. Spinel-structured $CuCr_2O_4$ black oxide pigment doped with various metals (Mn, Ni, Co, Al, Zn, and Sn) was found to absorb more solar radiation, and this discovery led to the development of a method to further enhance the pigment's solar selective feature. The other metal doping to copper chromite ($CuCr_2O_4$) are not as effective as manganese at producing highly sun absorptive colours. Spinel black oxides with the chemical formula $CuCr(2_x)Mn_xO_4$ were effectively synthesised, as shown by XRD analysis. Among the metal doped black oxides synthesised using hydrothermal synthesis, Mn-doped black oxide exhibits the greatest absorptivity (the lowest band gap value of 1.35 eV). Manganese is the sole dopant that reduces the reflectance peaks at 1 and 1.5 m in the light spectrum shown by copper chromium oxide, hence increasing the pigment's solar absorptivity. $CuCr_{(2x)}Mn_xO_4$ is doped with a variety of manganese concentrations (x = 0.1, 0.25, 0.5, 1, 1.5, 1.75, and 1.9). When doped with 100% (x = 1) manganese, solar absorbance increases to 0.9874, and the figure of merit (FOM) rises to 0.9284, indicating very selective solar absorption [24].

1.2 FERRITES:

Kasi Viswanath I. V. et al. have created several different types of nano-sized ferrites, including nickel ferrite, copper ferrite, zinc ferrite, nickel copper ferrite, and nickel copper zinc ferrite fine particles. By using the citrate-gel forerunner technique and calcining the ferrites at an 800°C temperature. Scanning electron microscopy (SEM) and X-ray diffraction (XRD) were used to analyse the precipitates that resulted (SEM). The crystal diameters of the ferrite powders were constructed between 20 and 65 nm at a temperature of 800°C, and the powders showed XRD line broadening [25].

Koseoglu Y. et al. have been manufactured by the manganese assisted nickel ferrite nanoparticles, $Mn_{0.2}Ni_{0.8}Fe_2O_4$, using a hydrothermal method with surfactant. X-ray diffraction studies, together with indications of magnetization and coercive field in the M-H curve's hotspot, determined that the crystal's size was 6 nm. As the heating rate was slowed, the sample's coercive field and magnetising field both increased, and the broad peak seen in ZFC identified the super-paramagnetic nature of the particles heated to a temperature barrier of 130 K and revealed semiconducting properties [26].

Nawal K. and Mukherjee S. developed nano-crystalline mixed ferrites by equilibrated lower entropy technique of manganese nickel ferrite particles having general formula $Mn_xNi_{1-x}Fe_2O_4$. Chemical co-precipitation produced a binary sequence of samples with 'x' varying from 0.0 to 0.5. The particles have a spinel shape and were 21-51nm in size [27].

Mund H. S. has described the $Co_{0.4}Mg_{0.6}Fe_2O_4$ nano-ferrites materials are created by employing self-combustion process without any external oxidising agents, and impact of forging temperature on structural attributes of these materials. X-ray diffraction (XRD) analysis revealed that the particle size of Co-Mg nano materials increased from 15 nm to 59 nm in diameter with an increase in forging temperature. Raman and Fourier transform infrared spectroscopy research was used to determine that spinel ferrite was structurally stable with the functional group [28].

Sagadevan S., Podder J., and Das I. produced $CoFe_2O_4$ nanoparticles using a hydrothermal technique. The XRD pattern validated the cubical structure. The diameters of the produced samples were reported in nanometres after SEM and TEM investigations verified their authenticity. The dielectric constant, dielectric loss, and alternating current (AC) conductivity of $CoFe_2O_4$-prepared materials are investigated as a function of frequency and temperature. The frequency increases of both the dielectric loss and the dielectric constant, but the dielectric constant decreases in the dielectric analysis reports, as well as increases in temperature and frequency of the alternating current electrical conductivity [29].

Zhou J. et al. Nickel ferrite ($NiFe_2O_4$) nanoparticles were successfully synthesized by the use of hydrothermal manner and characterized by X-ray diffraction (XRD) and transmission electron microscope (TEM) systems and also observed the effects of temperature for reaction completion, hold time and RH ratio i.e., isopropyl alcohol or water which gave $NiFe_2O_4$ nanoparticles at 60°C with 3 hours and finally crystallized by the same [30].

Radhe Shyam A. et al. have been revealed that the **a**lkylation of pyridine by methanol to methyl pyridine ensuing gap or phase in immovable bed reactor ranges from 473-723 K temperature over the $Zn_{1-x}Mn_xFe_2O_4$ (where x = 0, 0.25, 0.50, 0.75 and 1) ferro-spinel arrangement. It was observed that 2-picoline and 3-picoline were found to be major products in the systems having higher x values are greatly selective for the 2-picoline. 2-methylpyridine maximum yield of 67.6% with a selectivity of 79.5% and 17.5% of 3-methylpyridine with a selectivity of 20.5% was achieved over $MnFe_2O_4$ at a temperature of 673 K. The characterization catalyst has been completed by XRD, infrared spectroscopy and ammonia desorption methods [31].

Ameer Azam et al. reported a sol-gel combustion pathway was synthesized by nanosized particles of three metal oxides (ZnO, CuO, and Fe_2O_3) and described by X-ray diffraction, Fourier-transform infrared spectroscopy, and transmission electron microscopy techniques. The single-phase structure of all three nanomaterials was verified by X-ray diffraction outcomes. Particle sizes for ZnO, CuO, and Fe_2O_3 were found to be 18, 22, and 28 nm, respectively. To test their antibacterial efficacy against both Gram-negative bacteria (*Escherichia coli* and *Pseudomonas aeruginosa*) and Gram-positive bacteria (*Staphylococcus aureus* and *Bacillus subtilis*), used these nano-materials [32].

Heng-Hui Yu et al. reported the Spherolites with nanoscale M(II) substitutions (M = Fe, Mn, or Co; x = 0-1) in magnetically active $M_xFe_{3-x}O_4$ (M = Fe, Mn, or Co) have been effectively synthesized using a simple, robust, and time-saving microwave-assisted reflux approach in EG solvent without the inclusion of surfactants. During 30 min. of microwave heating, ferrite nanostructures emerge via an aggregation-based process. At room temperature, the magnetic nanostructured spherolites in their as-prepared form have a very large surface area and very strong magnetic characteristics [33].

Kalyani S., et al. described by controlling reaction temperature with microwave aided synthesis yields ferrite magnetic nanoparticles of various sizes. XRD, SAXS, VSM, TGA, DSC, and Fourier transform infrared spectroscopy were used to analyse iron oxide nanoparticles produced at 45 and 85°C (FTIR). At ambient temperature, iron oxide nanoparticles produced at 45 and 85°C were 10 and 13.8 nm, respectively, and superparamagnetic. Nanoparticles produced at 45 and 85°C had saturation magnetization values of 67 and 72 emu/g. Increased incubation temperature decreases supersaturation, increasing particle size and saturation magnetization levels. Iron oxide nanoparticles produced at 45 and 85°C have Curie temperatures of 561 and 566, respectively. The FTIR spectra of iron oxide nanoparticles produced at various temperatures showed the peaks of stretching bonds between octahedral and tetrahedral metal ions to oxide ions [34].

1.3 ALUMINATES:

Riahi-Madvaar, R et al. have been reported the synthesis of $SrAl_2O_4$ nanostructures using microwave irradiation and pomegranate juice was carried out in this research using an environmentally friendly approach. The raw materials were irradiated with 720-900 W for 6-10 min and subsequently calcined at 550°C for 5 hours, yielding $SrAl_2O_4$ nanocrystals. $SrAl_2O_4$ nanoparticles with improved characteristics in terms of shape and particle size have been created by using pomegranate juice as a dispersing and stabilizing agent. Morphology and particle size optimization were also investigated as a function of varying synthesis process factors including microwave power and reaction time. Produced $SrAl_2O_4$ nanoparticles were examined and characterized using X-ray diffraction and field emission-scanning electron microscopy [35].

Irosław Zawadzki prepared and reported the nanosized zinc aluminate $ZnAl_2O_4$ with a spinel structure and high specific surface area (220 m^2/g), microporosity, and narrow pore size distribution using microwave assisted hydrothermal technique. $Al_2(OH)_{6-x}(NO_3)_x$ and hydrated zinc acetate were the microwave–hydrothermal synthesis precursors. Unlike existing approaches, the proposed synthesis produces spinel phase quickly and without high temperature heating. XRD, TEM, SAED, SEM, DTA-TG, and textural analyses were used to describe the materials (surface area and porosity). $ZnAl_2O_4$ may also be useful for making thermally stable thin film coatings on planar surfaces [36].

Alexandre A. S. et al. have been the synthesis of $MeAl_2O_4$ with unique textural properties for example excessive large pores and high surface area was successfully accomplished by rational design of the synthetic route that permits single to minimize the entropy changes during phase conversion under the evolution of temperature. The high thermo-mechanical resistance of the $MeAl_2O_4$ and γ-Al_2O_3formed by using this method resulting the materials higher surface areas, high crystalline nature, larger pore volumes and larger pore sizes than the formation by another methods. Accumulation of Co^{++} lead to the highest decomposition temperature of the block copolymer followed by Ni^{++} and Cu^{++} counts. This type of synthesis strategy represents an improvement in the construction of transition metal aluminate phases with higher porosity and surface area; meanwhile these materials generally possess lower surface areas and volumes of stoma due to the high applied temperature to achieve the spinel phases. Furthermore, the boosted acid-base properties make these materials applicable as supports, adsorbents and catalysts [37].

Hamdy N. et al. produced spinel-structured blue nano cobalt-alumina pigments utilizing ceramic and sol gel techniques. This study created spinel-structured nanoscale $CoAl_2O_4$ and $Co_xMg_{1-x}Al_2O_4$ pigments using the ceramic technique. Magnesium was added to make more colours. XRD and TEM showed that the synthesized pigments had spinel structures with nano-sizes. Scherrer equation confirmed that the crystallite size of all samples was 20-40 μm. Magnesium lightens cobalt spinel pigment. These colours cover metallic surfaces well and hide them [38].

Li Y. et al. synthesized many spinel compositions using $MgO.nAl_2O_3$ (n = 0.5, 0.667, 0.85, 1, 1.25, 1.5, 1.75, 2.4) utilizing improved experimental solid-state process at 1600°C. XRD and SEM of the produced samples revealed single-phase non-stoichiometric spinels with spectroscopic n values from 0.667 to 1.5. As n grows, hardness and modulus decrease, implying that new compositions with better mechanical characteristics would be found in $n < 1$. Hence, the trial circumstances improve sample mechanical characteristics [39].

Abaide E. R. et al. reported a novel method to produce nano-particulate blue pigment of cobalt aluminate by emergent wetness impregnation of commercial alumina nano-particles with cobalt pioneer salt, monitored by drying and calcining the prepared nano-powders with the core structure $CoAl_2O_4/Al_2O_3$. The Co/Al ratio without stoichiometry produces great colours without changing the size of the original Al_2O_3 nanoparticle. The blue pigment produced by the $CoAl_2O_4$ shell is sufficient, however the molar cobalt precursor/Al_2O_3 ratio and calcination temperature may be adjusted [40].

Patil P. S. et al. Using glycine fuel and a sol-gel combustion heating method, the nano aluminate spinel $Ni_{1-x}Co_xAl_2O_4$ (x = 0.0, 0.25, 0.50, 0.75, 1.0) may be manufactured. Spinel structures of nickel aluminates, cobalt aluminates, and their varying constituents are calcined at high temperatures to create nanostructures. The influence of Co^{2+} ions on the $NiAl_2O_4$ force network plays a crucial role in the adaptation and development of cobalt-doped nickel aluminates' thermal, spectroscopic, structural, morphological, elementary, and finally catalytic properties. It has been shown that the produced aluminium content works well as a nano catalyst in the production of higher-yield organic molecules. When used, these techniques are tested for their ability to dissect the planned actions that led to the most common results [41].

Panda P. C. and Raj R. was shown by to be possible because precipitation in the poly-crystalline materials was not confined to the surface. The consistent precipitation of Al_2O_3

throughout the larger portion without the production of intermediate phases Due to volume contraction associated with precipitation of Al_2O_3 from spinel, precipitation inserted at existing grain boundaries facilitates pore materialization with high flexibility [42].

Sanjabi S. and Obeydavi A. produced $MgAl_2O_4$ nano powder spinel using modified sol-gel. The calcination temperatures from 700℃ to 900℃ were tuned to create $MgAl_2O_4$ spinel at 800℃. Meso-porous structure yielded 154 m^2g^{-1} surface area and 11nm crystallite size. FESEM and HRTEM micrographs showed that spinel $MgAl_2O_4$ powders were fine, homogeneous, and 12 nm by averaging 20 nm particle diameters. This method found nanometer-sized powders with ultra-fine particles, tiny crystal size, homogenous distribution, and high surface covering area [43].

Guo Z., Zheng J., Liu Y, and Chu W. produced nickel-based mixed metal oxide catalysts via double-layered hydroxide decomposition and fully characterized them. Upkeeps active nickel species catalyzed methane decomposition using the supplied ingredients. Hydrogen gas chemisorption showed that $Ni_{0.5}$Al-MMO and Ni1Al-MMO had 17.1 and 21.1 m^2/g Ni metallic surface extents, substantially greater than $Ni_{0.5}/Al_2O_3$ and Ni1 or Al_2O_3 saturated catalysts. XPS, XRD, and H_2-TPR showed that strong metal-support interaction reduced NiO concentration at active locations. Once Ni or Al ratios were increased to 2 and 3, Ni_xAl-MMO catalysts yielded 2.02 and 4.55 gc/gcat, compared to 1.36 and 1.29 for permeating Ni catalysts. Furthermore, because to adequate metal sustenance interfaces, MMO catalysts have more decreased Ni active sites for methane breakdown [44].

5. Concluding remarks with Discussion

In conclusion, ferrite, chromite, and aluminate nano materials have been extensively studied due to their unique properties and wide range of potential applications in various fields. The properties of these materials can be easily tuned by controlling the synthesis parameters, which offers a significant advantage over conventional materials. These tiny structures with sizes ranging from 1-100 nm have unique and incredible properties that make them perfect for a variety of applications. Advances in the synthesis processes and characterization techniques of these materials have enabled their development and optimization to fit different industrial and research applications. Chromite, ferrites, and aluminates contain transition metals that are magnetic – making them useful for creating high-strength magnets used in various electronic devices like hard drives and motors. The future research in the synthesis and application of these materials is expected to lead to the development of novel and advanced technologies with potential economic and environmental benefits. Advance efforts in the research and development of these materials will lead to more efficient synthesis and better understanding of their characteristics and properties, which will spur the growth of new industrial applications.

REFERENCES

[1] *Qing Zhao, Zhenhua Yan, Chengcheng Chen, and Jun Chen, Chem. Rev., 117, 15, **(2017)**, 10121-10211 doi.org/10.1021/acs.chemrev.7b00051.*

[2] *Walsh A., Wei S., Yan Y., Al-Jassim M.M., and Turner J.A., PhysicalReview, B 76, 165119.1-165119.9, **(2007)**.*

[3] *Christine Stella K., Samson Nesaraj A., Iranian Journal of Materials Science and Engineering, 7, 3-6, **(2010)**.*

[4] *Kim J. W., Shin P. W., Lee M. J., Lee S. J., Journal of Ceramic Processing and Research, 7, 117, **(2006)**.*

[5] *Wang Y., Rainforth W. M., Jones H., Lieblich M., Wear, 251, 14-21, **(2001)**.*

[6] *Feng Y. C., Geng L., Zheng P. Q., Zheng Z. Z., Wang G. S., Mater. Des., 29, 20-23, **(2008)**.*

[7] *Zhou Yang, Yu Zhenyang, Zhao Naiqin, Shi Chunsheng, Liu Enzuo, Du Xiwen, He Chunnian, Mater. Des., 46, 724,* ***(2013)***.

[8] *Uju W. A., Oguocha. I. N. A., Mater. Des., 33, 503,* ***(2012)***.

[9] *Mohammadpour Amini M., Torkian L., Matter. Lett., 57, 639,* ***(2002)***.

[10] *Yamakawa A., Hashiba M., Nurishi Y., J. Mater. Sci., 24, 1491,* ***(1989)***.

[11] *Fei W. D., Hu M., Yao C. K., Mater. Chem. Phys., 77, 882,* ***(2003)***.

[12] *Arean C. O., Mentruit M. P, Lopez A. J., Parra J. B., Coll. Surf. A, 180, 253,* ***(2001)***.

[13] *Meyer F., Hempelmann R., Mathur S., Veith M., J. Mater. Chem., 9, 1755,* ***(1999)***.

[14] *Jeevanandam P., Koltypin Yu, Gedaanken A., Mater. Sci. Eng. B, 90. 125,* ***(2002)***.

[15] *Abdolmohammadi Shahrzad and Dahi-Azar Saman, J Heterocyclic Chem., 1-8,* ***(2021)***. *doi: 10.1002/jhet.4347.*

[16] *Javad Safaei-Ghomi, Zeinab Akbarzadeh, Bahareh Khojastehbakht-Koopaei, RSC Advances, 1(3), 1-17,* ***(2013)***.

[17] *Shojaei Abdollah Fallah, Farhad Shirini and Elaheh Hedayati, Comparison of selective oxidation of aromatic alcohols using copper (II) chromite-titanium dioxide nanocomposite at reflux, light irradiation and microwave conditions, Inorganic and Nano-Metal Chemistry,* ***(2017)***. *doi: 10.1080/24701556.2017.1284093.*

[18] *Saeed, M.; Rani, M.; Batool, K.; Batool, H.; Younus, A.; Azam, S.; Mehmood, A.; Haq, B.; Alshahrani, T.; Ali, G., J. Compos. Sci. 5, 247,* ***(2021)***. *https://doi.org/10.3390/ jcs5090247.*

[19] *Shankha S. Acharyya, Shilpi Ghosh, and Rajaram Bal, Ind. Eng. Chem. Res.,* ***(2014)***. *doi.org/10.1021/ie5026634.*

[20] *Aparecida M. Kawamoto, Luiz Claudio Pardini, and Luis Claudio Rezende, Aerospace Science and Technology, 8, 591–598,* ***(2004)***.

[21] *Safaei-Ghomi, J., Akbarzadeh, Z., & Khojastehbakht-Koopaei, B., RSC Advances, 5(37), 28879–28884,* ***(2015)***. *doi:10.1039/c5ra01915j .*

[22] *Manoharan S. S. and Patil K.C., Communications of the American Ceramic Society, 75(4), 1012-1015,* ***(1992)***.

[23] *Zhigaikina I. A., Nikolaeva T. D., Suponitskii Yu. L., and Polyak B. I., Glass and Ceramics, 55 (5-6), 182-185,* ***(1998)***.

[24] *Yongjoon Youn, John Miller, Kathy Nwe, Kyung-Jun Hwang, Chulmin Choi, Youngjin Kim, and Sungho Jin, ACS Applied Energy Materials, 2 (1), 882-888,* ***(2019).*** *DOI: 10.1021/acsaem.8b01976.*

[25] *KasiViswanath I. V., Murthy Y. L. N., Tata K.andSingh R., Int. J. Chem. Sci., 11(1), 64-72,* ***(2013)***.

[26] *Koseoglu Y., Bay M., Tan M., Baykal A., Sozeri H., Topkaya R. And Akdogan N., J. Nanopart Res., (13), 2235-2244,* ***(2011)***.

[27] *Nawal K. and Mukherjee S., International Journal of Scientific and Research Publications, 4(1),* ***(2014)***.

[28] *Mund H. S., JOJ Material Sci, 2(2),* ***(2017)***.

[29] *Sagadevan S., Podder J., Das I., Springer Proceedings in Physics, 189,* ***(2017)***, *145-152.*

[30] *Zhou J.,Ma J., Sun C., Xie L., Zhao Z., Yonggang Wang H., TaoJ.and Zhu X., J. Am. Ceram. Soc., 88 (12), 3535-3537,* ***(2005)***.

[31] *RadheShyam A., Dwivedi R., ReddyV. S., Chary K. V. R. and Prasad R., The Royal Society of Chemistry Green Chemistry, 4, 558-561,* ***(2002)***.

[32] *Ameer Azam, Arham S Ahmed, Mohammad Oves, Mohammad S Khan, Sami S Habib, Adnan Memic, Int J Nanomedicine, 7: 6003-6009,* ***(2012)***. *doi: 10.2147/IJN.S35347.*

[33] *Heng-Hui Yu, Qian-Lin Wang, Yao Chen, Yan Wang, Jia-Hong Wang, Materials Letters, 278, 128431,* ***(2020)***. *doi.org/10.1016/j.matlet.2020.128431.*

[34] *Kalyani S, Sangeetha J, Philip J., J Nanosci Nanotechnol. Aug;15(8):5768-74,* ***(2015)***. *doi: 10.1166/jnn.2015.10274. PMID: 26369150.*

[35] *Riahi-Madvaar, R., Taher, M.A. and Fazelirad, H., Appl Nanosci* ***7****, 913–917,* ***(2017)****. doi.org/10.1007/s13204-017-0628-1.*

[36] *Iroslaw Zawadzki, Solid State Sciences, 8(1), 14-18,* ***(2006)****. doi.org/10.1016/j.solidstatesciences.2005.08.006.*

[37] *Alexandre A. S., Goncalves, Maria J. F. Costa, Zhang L., Ciesielczyk F. and Jaroniec M., Chem. Mater.,30, 436-446,* ***(2018)****.*

[38] *Hamdy N., Elgazwy A. S. H., Mahmoud W. H., Selim M. M., Egy. J. Pure and Appl. Sci., 039-043,* ***(2012)****.*

[39] *Li Y., Yang D., Liu C., Yang P., Mu P., Wen J., Chen S. and Li Y., Ceramics International,* ***(2018)****. doi/10.1016/j.ceramint.2018.05.145.*

[40] *Abaide E. R., Anchieta C. G., Foletto V. S., Reinehr B., Nunes L. F., Kuhna R. C., Mazutti M. A., Foletto E. L., Materials Research., 18(5), 1062-1069,* ***(2015)****. (doi/10.1590/1516-1439.031415).*

[41] *Prakash S. Patil, Ravindra S. Dhivare, Sunil R. Mirgane, Bharat G. Pawar, Tanaji R. Mane, Macromol. Symp., 393, 2000163, 1-7,* ***(2020)****.*

[42] *Panda P.C. and Raj R., J. Am. Ceram. Soc., 69(5), 365-73,* ***(1986)****.*

[43] *Sanjabi S., Obeydavi A., Journal of Alloys and Compounds,* ***(2015)****. doi/10.1016/j.jallcom.2015.05.107.*

[44] *Guo Z., Zheng J., Liu Y and Chu W., Applied Catalysis,* ***(2010)****. doi./10.1016/j.apcata.2018.01.031.*